Pion Production by Pions*

WALTON A. PERKINS, III, JOHN C. CARIS, ROBERT W. KENNEY, AND VICTOR PEREZ-MENDEZ
Lawrence Radiation Laboratory, University of California, Berkeley, California

(Received October 7, 1959)

A liquid hydrogen target was bombarded by negative pions of energies 260, 317, 371, and 427 Mev. Positive pions from the reaction $\pi^-+p\rightarrow\pi^++\pi^-+n$ were detected by the use of a counter telescope, that selected the π^+ by its characteristic π-μ decay. With the 260-Mev beam, π^+ mesons were counted at 90° in the laboratory system. At 317, 371, and 427 Mev, the differential cross section was measured for π^+ mesons emitted at 60°, 90°, 125°, and 160° in the center-of-mass system. The angular distributions are nearly isotropic at 317 and 371 Mev but are peaked forward at 427 Mev. The total cross sections are 0.14±0.10 mb at 260 Mev, 0.71±0.17 mb at 317 Mev, 1.93±0.37 mb at 371 Mev, and 3.36±0.74 mb at 427 Mev. These results indicate a much larger cross section than the theoretical prediction based on the static model. Reasonable agreement can be obtained by the inclusion of a pion-pion interaction in the production mechanism.

INTRODUCTION

THE following reactions for single-meson production:

$$\pi^++p\rightarrow\pi^++\pi^++n,$$
$$\pi^++p\rightarrow\pi^0+\pi^++p,$$
$$\pi^-+p\rightarrow\pi^0+\pi^-+p,$$
$$\pi^-+p\rightarrow\pi^++\pi^-+n,$$

have been studied in emulsions,[1–5] in hydrogen diffusion cloud chambers,[6–8] in bubble chambers,[9–11] and recently with counters.[12] Most of this work was done in the laboratory (lab)-system kinetic-energy region near 1 Bev for the incident pions.

Theoretical calculations for the above processes by Barshay,[13] Franklin,[14] Rodberg,[15] and Kazes[16] are an extension of the Chew-Low formalism for meson scattering to the process of meson scattering with production. This theory calculates the p-wave production in the one-meson approximation with an extended stationary nucleon and is not expected to be applicable at high energy. Indeed, if the results of the theory are extrapolated to high energy,[15] they predict cross sections which are much too small.

There is some evidence[12] of a disagreement with theory in the energy region near threshold, but the results are not conclusive. With this in mind, we undertook the study of the process $\pi^-+p\rightarrow\pi^++\pi^-+n$ in the energy region from 260 to 430 Mev. A unique signature for this reaction is provided by the π^+ meson in the final state, and it was unambiguously identified by its characteristic π-μ decay. The reactions in which two secondary pions are produced can be neglected, because the highest energies are just barely above the energetic threshold of 360 Mev, and even at higher energies these cross sections are very small.[10]

A large difference between experiment and theory might show a need for the inclusion of nucleon recoil or a pion-pion interaction in the theory. However, in this energy region one does not expect nucleon recoil to be important enough to account for any large discrepancy.

EXPERIMENTAL ARRANGEMENT AND METHOD

A diagram of the experimental arrangement is shown in Fig. 1. The 730-Mev proton beam of the Berkeley synchrocyclotron struck an internal beryllium target which was 2 in. thick in the beam direction. Negative pions were deflected by the cyclotron magnetic field and passed out of the vacuum tank through a thin aluminum window. The pions were next focused by a two-section quadrupole magnetic lens with an aperture of 8 in.

After traversing an 8-ft iron collimator, the pion beam was bent through 55° by a wedge magnet with equal horizontal and vertical focusing. The three-section 8-in. quadrupole magnet was used for fine adjustments in focusing the beam.

A π^- beam of intensity equal to or greater than 10^4 per second through a 2-in. diam counter (Counter 2 in Fig. 1) was available at all the energies used. The kinetic energies of the pion beams were 260, 317, 371, and 427 Mev, and the energy spread was ±2.5%. Muon contaminations, decreasing from 11±2% at 260 Mev

* This work was done under the auspices of the U. S. Atomic Energy Commission.

[1] J. Crussard, W. D. Walker, and M. Koshiba, Phys. Rev. **94**, 736 (1954).
[2] M. Blau and M. Caulton, Phys. Rev. **96**, 150 (1954).
[3] W. D. Walker and J. Crussard, Phys. Rev. **98**, 1416 (1955).
[4] Walker, Hushfar, and Shephard, Phys. Rev. **104**, 526 (1956).
[5] W. D. Walker, Phys. Rev. **108**, 872 (1957).
[6] Eisberg, Fowler, Lea, Shephard, Shutt, Thorndike, and Whittemore, Phys. Rev. **97**, 797 (1955).
[7] Maenchen, Fowler, Powell, and Wright, Phys. Rev. **108**, 850 (1957).
[8] Blevins, Block, and Leitner, Phys. Rev. **112**, 1287 (1958).
[9] A. R. Erwin and J. K. Kopp, Phys. Rev. **109**, 1364 (1958).
[10] Lee Baggett, University of California Radiation Laboratory Report UCRL-8302, May, 1958 (unpublished).
[11] Crittenden, Scandrett, Shephard, Walker, and Ballam, Phys. Rev. Letters **2**, 121 (1959).
[12] V. G. Zinov and S. M. Korenchenko, Zhur. Eksptl. i Teoret. Fiz. **34**, 301 (1958) [translation: Soviet Phys.-JETP **34(7)**, 210 (1958)].
[13] S. Barshay, Phys. Rev. **103**, 1102 (1956).
[14] J. Franklin, Phys. Rev. **105**, 1101 (1957).
[15] L. S. Rodberg, Phys. Rev. **106**, 1090 (1957).
[16] E. Kazes, Phys. Rev. **107**, 1131 (1957).

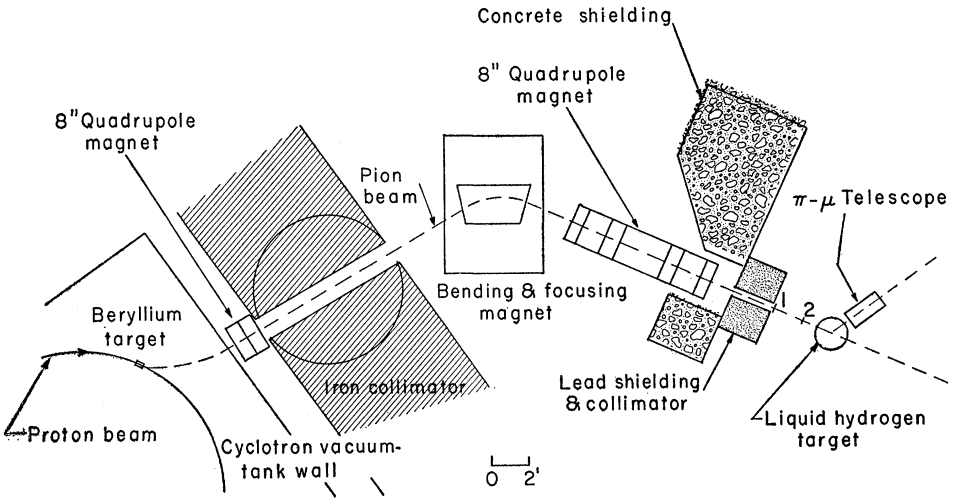

FIG. 1. Diagram of experimental arrangement.

to $4\pm2\%$ at 427 Mev, were determined from range curves (a typical integral range curve is shown in Fig. 2 for 371 Mev). Upper limits for the electron contamination, obtained by calculation, were 5, 3, 2, and 2% for 260, 317, 371, and 427 Mev, respectively. No electron-contamination correction was applied to the data, and the upper limits gave an uncertainty that was negligible in comparison with the statistical accuracy.

The pion beam was incident upon the liquid-hydrogen target after traversing the two beam-defining counters as shown in Fig. 3. The 4.5-in. diam Mylar end windows of the vacuum chamber provided a thin low-Z material in the direct beam. The liquid-hydrogen container was made of 0.02-in. thick, 5-in. wide Mylar sheet held by copper top and bottom plates to the shape shown in Fig. 3. This target was similar to those described by Hickman et al.[17]

The counter telescope was mounted on a dolly and could be conveniently rotated to any angle. The desired π^+ lab energy was observed by placing the appropriate copper absorber between Counters 3 and 4 (see Fig. 3), and also before Counter 3 for the high-energy pions.

ELECTRONICS

A block diagram of the electronics is shown in Fig. 4. The identification of the π^+ mesons was made by a

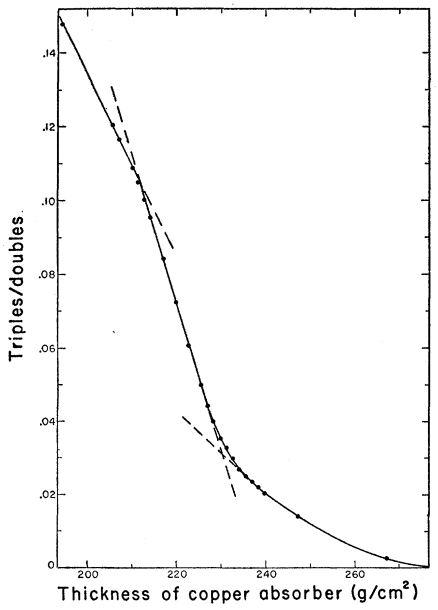

FIG. 2. Integral range curve for 371-Mev negative-pion beam.

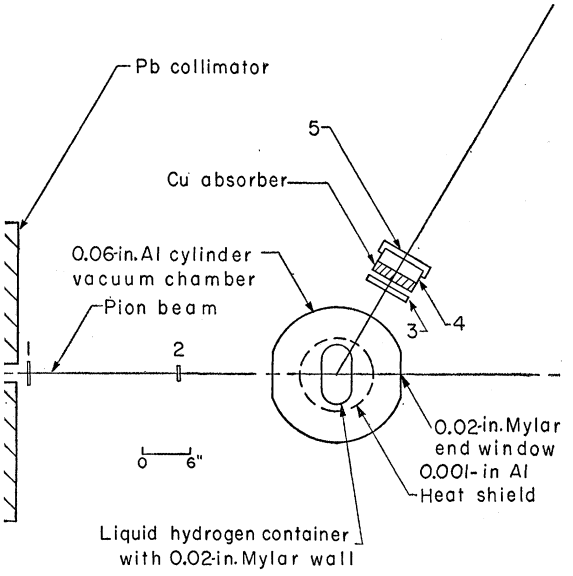

FIG. 3. Diagram showing details of hydrogen target and counter arrangement.

[17] Hickman, Kenney, Mathewson, and Perkins, University of California Radiation Laboratory Report UCRL-8662, February 19, 1959 (unpublished).

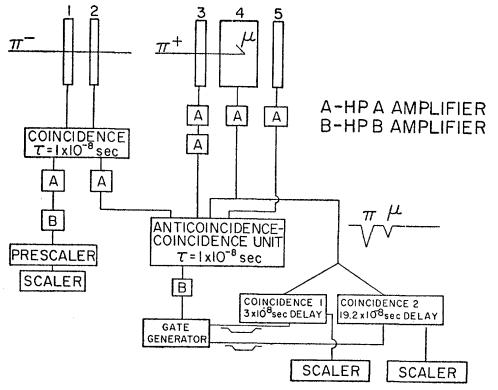

FIG. 4. Block diagram of electronics for monitor and π-μ telescope.

delayed π-μ coincidence technique. A detailed description of the basic electronic equipment required has been reported elsewhere.[18] In this experiment the coincidence 12345 initiated a gate of 6×10^{-8}-sec duration, delayed approximately 3×10^{-8} sec relative to the initiating pulse. The coincidence between the gate and delayed pulse in Counter 4 was registered on a scaler. When this occurred, presumably a π^- meson traversed Counters 1 and 2 and entered the H_2 target, producing the π^+ meson. The positive pion passed through Counter 3 and stopped in Counter 4, generating the 6×10^{-8}-sec gate pulse. Then the μ^+ from the π^+ decay gave a delayed pulse that made a coincidence with the gate.

However, it was possible for two random particles or a μ-e decay to simulate this effect. The accidental and μ-e decay coincidences were monitored by the use of an identical coincidence channel in which the gate delay was set at 19.2×10^{-8} sec (i.e., delayed 3 rf synchrocyclotron pulses more than first gate).

COUNTER-TELESCOPE CALIBRATION

The absolute efficiency of the counter telescope was determined by using a magnetically analyzed beam of positive pions. The two experimental points in Fig. 5

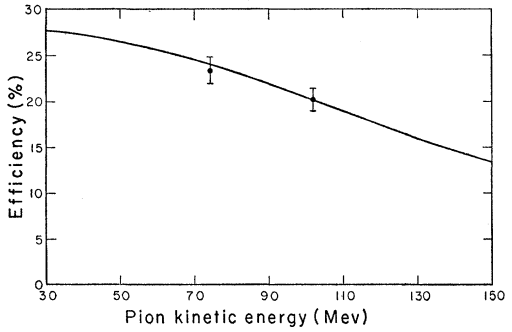

FIG. 5. Efficiency of π-μ telescope as a function of the kinetic energy of the stopping pion.

[18] W. Imhof, R. Kalibjian, and V. Perez-Mendez, Rev. Sci. Instr. **29**, 476 (1958).

represent the number of telescope counts for an incident π^+ meson as measured in the π^+ beam.

The efficiency, which is the product of three factors (a) delay, (b) absorption, and (c) multiple Coulomb scattering, was also determined by obtaining these three factors separately. The efficiency due to delay, which was measured experimentally, is the fraction of π^+ mesons that decays into muons during the time in which the muon pulses can make a coincidence with the gate. The absorption correction was calculated by the use of experimental cross sections.[19,20] The multiple Coulomb scattering correction (6% or less) was based on the geometrical calculations of Sternheimer[21] and included the energy loss consideration of Eyges.[22] Combining these three factors, we obtained the efficiency, which is shown as the solid line in Fig. 5.

RESULTS AND CORRECTIONS

Accidental counts in the π-μ telescope were monitored concurrently with the real counts. During the experiment, the ratio of accidental to real counts was between $\frac{1}{4}$ and 1.

Another correction had to be applied because of "beam bunching." Because of the high intensity π^- beams used, occasionally two pions bombarded the liquid-hydrogen target during the same rf synchrocyclotron pulse. When this occurred, only one count was registered by the monitor counters, whereas each π^- meson was capable of producing a π^+ meson. This correction was directly proportional to the beam intensity and was less than $(7\pm2)\%$ for all intensities used.

A correction was made for π^+ mesons decaying between the target and counter telescope. The magnitude of this correction varied from 2 to 6%, depending upon the π^+ meson's kinetic energy.

The data analysis was complicated by the geometrical conditions (i.e., thick target and large solid angle subtended by counter telescope at the target) used to obtain reasonable counting rates. The effective solid angle subtended by the counter telescope was calculated by an integration over the elements of target volume weighted by the beam shape, and the elements of counter area. The method used was similar to that presented by Anderson *et al.*[23] for a rectangular block target.

Measurements were taken for π^+ mesons emitted at 60°, 90°, 125°, and 160° in the center-of mass (c.m.) system for incident π^- kinetic energies of 317, 371, and 427 Mev. For a π^- kinetic energy of 260 Mev, only a single measurement was made at 90° in the lab system.

Since we are dealing with a three-body final state in

[19] D. Stork, Phys. Rev. **93**, 868 (1954).
[20] R. Martin, Phys. Rev. **87**, 1052 (1952).
[21] R. M. Sternheimer, Rev. Sci. Instr. **25**, 1070 (1954).
[22] L. Eyges, Phys. Rev. **74**, 1534 (1948).
[23] H. L. Anderson, W. C. Davidon, M. Glicksman, and U. E. Kruse, Phys. Rev. **100**, 279 (1955).

the reaction under study ($\pi^-+p\rightarrow\pi^++\pi^-+n$), the π^+ in the c.m. system can have any energy from zero to some maximum energy. This maximum energy depends only on T_1, the kinetic energy of the incident π^- meson in the laboratory system. For a π^+ emitted at some angle θ^* in the c.m. system, its lab angle θ will depend on T^*, its kinetic energy in the c.m. system. Therefore, to count π^+ mesons at one c.m. angle and several c.m. energies, it is necessary to use several lab angles. The differential cross section as a function of π^+ angle and kinetic energy is related to the experimental data by the formula

$$d^2\sigma/d\Omega^*dT^* = Y(\theta,T)\left[nt(1+\alpha)\frac{A}{d^2}\eta(1-\epsilon)(d\Omega^*/d\Omega)\Delta T^*\right]^{-1}.$$

Here $Y(\theta,T)$ is the net number of π^+ mesons (target full minus target empty) counted per incident π^- meson. This factor has been corrected for accidentals and beam bunching. The quantity nt is the number of hydrogen nuclei per square cm of target area. The mean target thickness was 4.320 in., and the difference in density between liquid hydrogen and hydrogen gas was determined to be 0.069 g/cm^3, resulting in 4.565×10^{23} nuclei/cm^2. The term $(1+\alpha)A/d^2$ is the effective solid angle subtended by the counter telescope in the laboratory system. In this experiment α varied with the angle from 0 to 7%. The efficiency of the counter telescope is η (see Fig. 5). The fraction of the pions that decay between the hydrogen target and the counter telescope is represented by ϵ. The solid angle transformation from the c.m. to lab system is $d\Omega^*/d\Omega$, ΔT^* is the c.m. energy-acceptance band for Counter 4.

TABLE I. Differential cross sections with respect to π^+ angle and energy.

	θ^* (deg)	T^* (Mev)	ΔT^* (Mev)	$(d^2\sigma/d\Omega^*dT^*)$ (μb/sr-Mev)
$T_1=260$ Mev, $T_{max}^*=57.1$ Mev	115.2	45.4	21.4	0.21±0.11
$T_1=317$ Mev, $T_{max}^*=91.3$ Mev	63.0	36.7	11.8	0.846±0.31
	90.0	28.6	16.1	0.853±0.19
	91.3	48.3	14.9	0.794±0.20
	89.3	62.1	13.1	0.770±0.24
	125.1	52.9	23.5	0.592±0.15
	122.6	73.6	18.5	0.447±0.24
	158.5	73.3	32.9	0.745±0.18
$T_1=371$ Mev, $T_{max}^*=122.1$ Mev	59.7	40.9	10.5	2.05±0.46
	60.0	74.3	10.3	1.21±0.27
	60.1	103.6	9.5	0.59±0.35
	92.1	34.5	15.5	1.98±0.33
	90.0	57.9	13.4	1.55±0.40
	90.1	78.8	12.4	0.91±0.29
	90.1	104.3	12.4	0.88±0.24
	127.2	55.4	23.9	1.77±0.27
	124.5	76.4	18.8	1.32±0.43
	125.1	103.3	17.6	0.93±0.24
	159.3	77.9	34.1	1.38±0.25
	160.0	109.0	26.0	0.42±0.30
$T_1=427$ Mev, $T_{max}^*=152.6$ Mev	60.6	43.0	10.0	2.88±0.45
	60.3	88.9	9.5	2.93±0.50
	90.3	45.0	13.4	2.17±0.48
	90.3	90.0	12.0	2.61±0.53
	90.4	124.5	11.6	1.01±0.42
	125.3	57.6	23.7	1.55±0.32
	125.3	111.4	17.0	1.26±0.26
	160.2	82.6	37.0	1.65±0.39

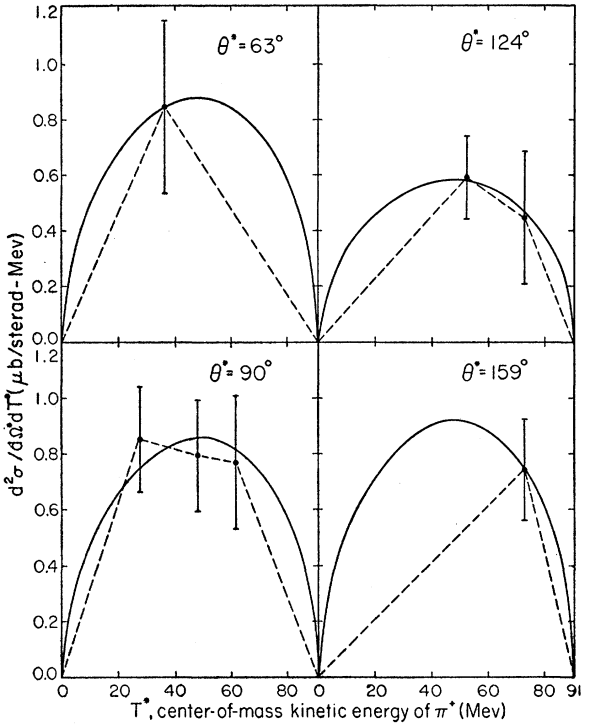

FIG. 6. Differential cross section for $\pi^-+p\rightarrow\pi^++\pi^-+n$ as a function of π^+ kinetic energy for incident π^- kinetic energy of 317 Mev and π^+ c.m. angles of 63°, 90°, 124°, and 159°. See text for explanation of various curves.

The experimental results for $d^2\sigma/d\Omega^*dT^*$ are presented in Table I. Curves of $d^2\sigma/d\Omega^*dT^*$ versus T^* are shown in Figs. 6 through 8. The solid line is the rela-

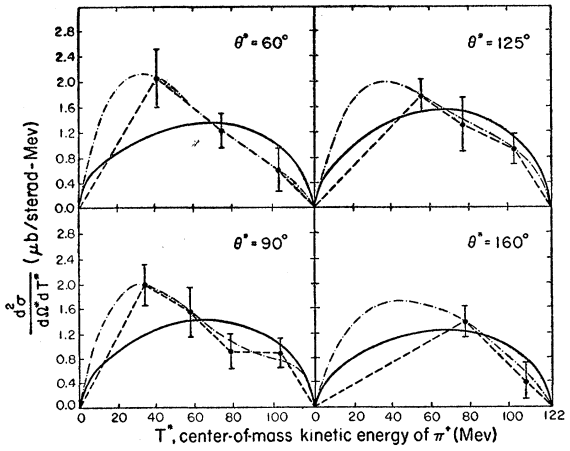

FIG. 7. Differential cross section for $\pi^-+p\rightarrow\pi^++\pi^-+n$ as a function of π^+ kinetic energy for incident π^- kinetic energy of 371 Mev and π^+ c.m. angles of 60°, 90°, 125°, and 160°. See text for explanation of various curves.

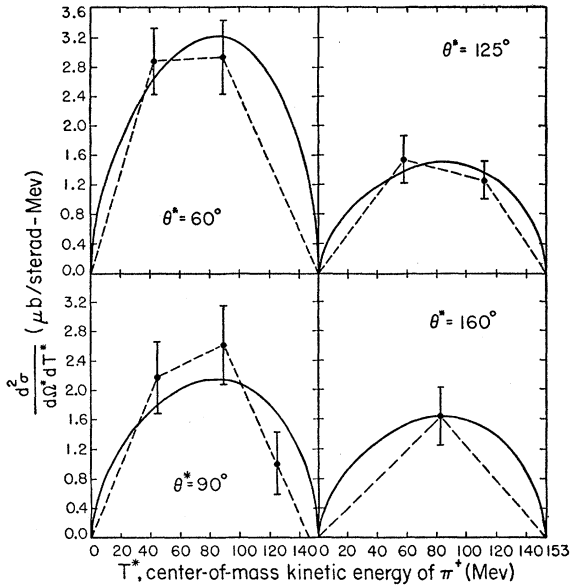

FIG. 8. Differential cross section for $\pi^-+p\rightarrow\pi^++\pi^-+n$ as a function of π^+ kinetic energy for incident π^- kinetic energy of 427 Mev and π^+ c.m. angles of 60°, 90°, 125°, and 160°. See text for explanation of various curves.

tivistic phase-space curve as given by Block.[24] The heights of the phase-space curves were determined by minimizing the weighted sum of the squares of the differences between the calculated and experimental values.

The statistical phase-space curves fit the data adequately for incident energies of 317 and 427 Mev, but the phase-space calculation predicts too few low-energy π^+ mesons at 371 Mev (see Fig. 7). In order to obtain the angular differential cross section, an integration was performed over the energy of the π^+ meson. The phase-space curves were used for 317 and 427 Mev, while the dash-dot curves were used for 371 Mev. The dashed curves were used to estimate a lower limit for the total cross sections.

TABLE II. Differential cross section as a function of π^+ angle.

T^* (Mev)	θ^* (deg)	$d\sigma/d\Omega^*$ (μb/sr)
317	63	62±23
317	90	60.2±9
317	124	41.0±9
317	159	64.4±16
371	60	154±19
371	90	152±18
371	125	165±20
371	160	145±26
427	60	369±42
427	90	245±35
427	125	173±25
427	160	189±45

Table II gives $d\sigma/d\Omega^*$ resulting from the integration. The errors listed are statistical only and do not include the errors involved in integration over π^+ energy.

The angular differential cross sections as a function of the c.m. angle for the π^+ meson are shown in Figs. 9 through 11. Least-squares fits to the experimental points were made by assuming a polynomial in $\cos\theta^*$. The curve of the form $d\sigma/d\Omega^*=a_0+a_1\cos\theta^*$ is shown

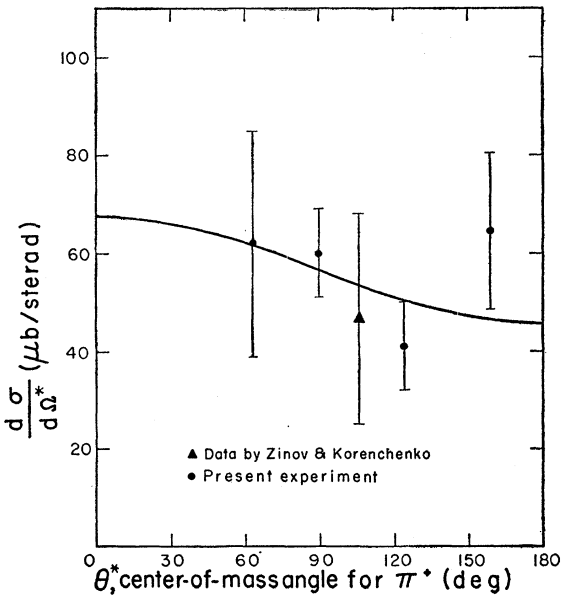

FIG. 9. Angular differential cross section for a π^+ meson for an incident π^- meson of 317-Mev energy.

[24] M. Block, Phys. Rev. **101**, 796 (1956).

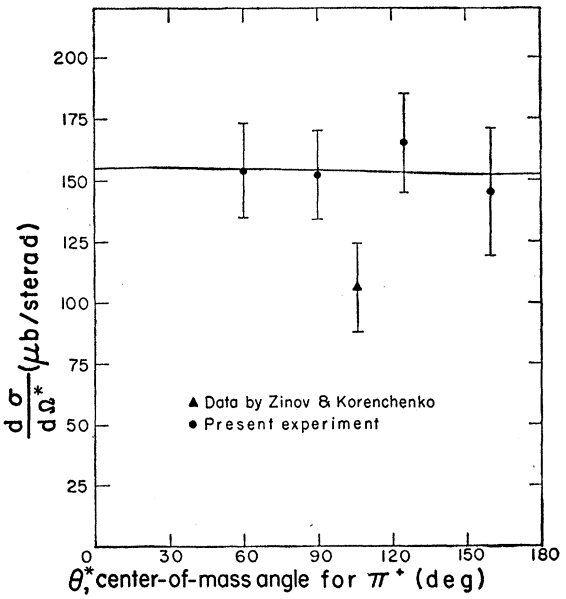

FIG. 10. Angular differential cross section for a π^+ meson for an incident π^- meson of 371-Mev energy.

as the solid line in Figs. 9–11. At 317 and 371 Mev, a curve of the form $d\sigma/d\Omega^*=a_0$ would also fit the data. The data of Zinov and Korenchenko,[12] shown for comparison only and not used in the least-squares fitting, was obtained with counters in a quite different manner.[25]

Another integration was performed in order to obtain the total cross sections. For 260 Mev, an isotropic differential cross section was assumed. The results are listed in Table III, with the experimental errors representing the combined errors of counting statistics and integration over π^+ angle and energy.

Total cross sections as a function of the incident π^- kinetic energy are shown in Fig. 12. The theoretical curves will be discussed in the next section. The error due to uncertainty in the efficiency of the counter telescope was estimated to be 6%. This and the smaller errors due to uncertainty in beam contamination and other corrections were negligible in comparison with the statistical errors and the uncertainty in the shape of π^+ energy spectrum. By using the dashed curves shown in Figs. 6–8 and folding in the statistics, we obtained the standard deviations given in Table III.

TABLE III. Total cross sections for $\pi^-+p\rightarrow\pi^++\pi^-+n$.

T_1 (Mev)	σ (mb)
260	0.14±0.10
317	0.71±0.17
371	1.93±0.37
427	3.36±0.74

DISCUSSION

The dashed-dot curve in Fig. 12 is the theoretical prediction given by Franklin.[14] The dashed curve is the theoretical prediction of Kazes[16]; Rodberg's prediction for this cross section is even smaller.[15] All of these predictions are based on the static model, and the variation in the result is caused by the different approximations used. Because of his use of the Born approximation, Franklin's earlier results do not satisfy the unitarity condition in the one-meson approximation. The results of Rodberg and Kazes, however, satisfy unitarity in the one-meson approximation and therefore are probably a more accurate interpretation of the static-model prediction.

Using the more recent theoretical results,[15,16] we note a systematic discrepancy of a factor of ten between

[25] The π^+ and π^- from $\pi^-+p\rightarrow\pi^++\pi^-+n$ and 70% of the π^- mesons from $\pi^-+p\rightarrow\pi^-+\pi^0+p$ were counted for $\theta^*=106°$ and $T^*\gtrsim T_{\max/2}{}^*$. In order to obtain the plotted points, it was assumed that the cross sections for both reactions were equal and $d^2\sigma/d\Omega^*dT^*$ was symmetrical about $T^*=T_{\max}{}^*/2$. The assumption of equal cross sections is not critical because the ratio of detection efficiencies for $\pi^-+p\rightarrow\pi^++\pi^-+n$ to $\pi^-+p\rightarrow\pi^-+\pi^0+n$ is 2/0.7. When one considers the assumptions involved, the agreement between the two sets of data is quite good.

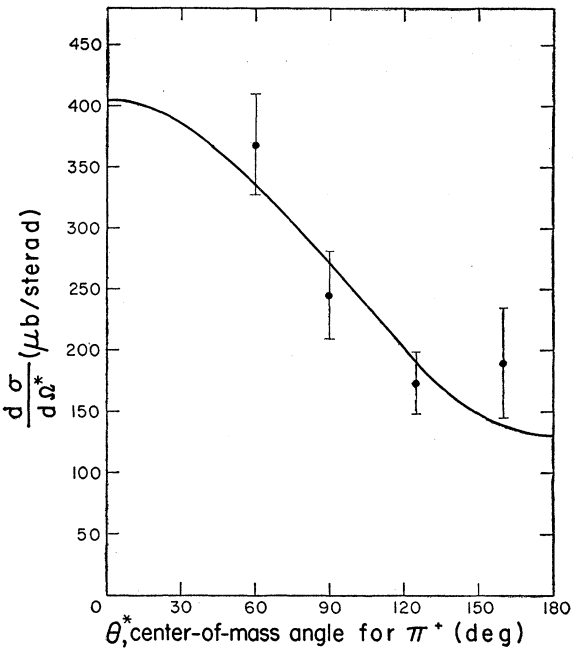

FIG. 11. Angular differential cross section for a π^+ meson for an incident π^- meson of 427-Mev energy.

results from experiment and static-model theory. The effect of including nucleon recoil in the calculations of the total cross sections is believed to be too small in

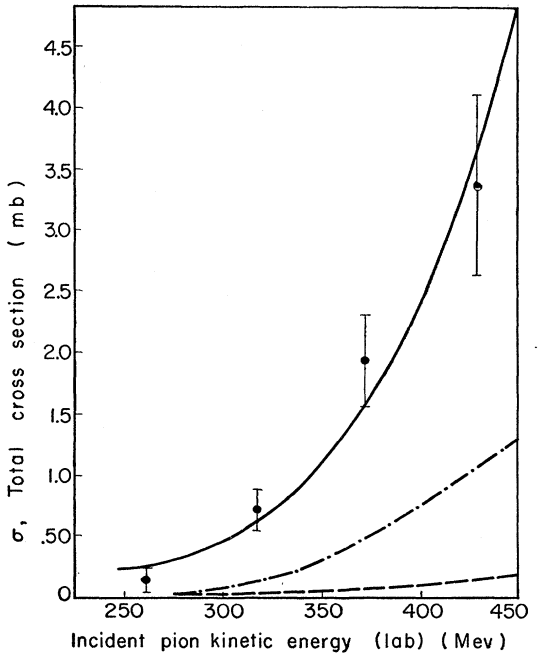

FIG. 12. Total cross section for $\pi^-+p\rightarrow\pi^++\pi^-+n$ as a function of the π^+ kinetic energy in the laboratory system. The solid curve is the theoretical result of Rodberg[22] based on the pion-pion interaction model. The dashed and dot-dashed curves are the theoretical predictions based on the static model by Kazes[16] and Franklin,[14] respectively.

this energy region to account for this large a discrepancy.[26]

The existence of a pion-pion interaction has been postulated to explain the nucleon structure[27] and the peak[28–30] in the π^--proton total cross section near 1 Bev. The direct interaction of the incident pion and a virtual pion in the meson cloud surrounding the nucleon could contribute significantly to the production of an extra pion in pion-nucleon collisions. The effect of a pion-pion interaction on the production cross section is discussed by Barshay[31] and more specifically by Rodberg[32] in connection with the particular reaction under study here. The solid line in Fig. 12 shows a fit to the experimental data by Rodberg[32] corresponding to physically plausible pion-pion phase shifts. At very high incident energies where the momentum of the virtual pion is much less important than near threshold, the qualitative predictions for the energy and angular distributions are: (a) the pions in the final state should be in the high energy region of their available phase space and go forward in the π^--p c.m. system, (b) the nucleon should act as a spectator, receiving only a small recoil momentum and going backward in the c.m. system. At 4.5 Bev the general features of effects (a) and (b) have been observed.[5]

For incident-pion energies near threshold, the momentum of the virtual pion tends to obscure these effects and the nucleon receives a momentum comparable with that of the incident pion. For this reason no differentiation could be made between the pion-pion interaction "model" and the static model on the basis of our measured π^+ energy spectrum.

The angular differential cross section (see Figs. 9 through 11) are nearly isotropic at 317 and 371 Mev, but peaked forward at 427 Mev. Apparently fore-aft asymmetry predicted at high energies[32] is washed out at the lower energies of 317 and 371 Mev by the momentum of the virtual pion but appears at the higher energy of 427 Mev.

Our results combined with those obtained by Zinov and Korenchenko[12] indicate that the ratio

$$(\pi^-+p\rightarrow\pi^++\pi^-+n)/(\pi^-+p\rightarrow\pi^-+\pi^0+p)$$

is probably 1 or greater. At 810 Mev the measured ratio[10] is 2.49. The static model predicts that the ratio should be about $\frac{1}{3}$,[14,16] while the pion-pion interaction model predicts about 2/1,[28,29,32] which is in better agreement with the experimental results.

ACKNOWLEDGMENTS

We are indebted to Professor A. C. Helmholz for his guidance and encouragement throughout this work. The assistance of Dr. Edward Knapp in the earlier phases and Lester Goodwin in the later stages of this experiment is greatly appreciated. We wish to thank James Vale and the cyclotron crew for their assistance and cooperation during the experimental work.

[26] Leonard S. Rodberg, Department of Physics, University of Maryland, College Park (private communication).
[27] W. R. Frazer and J. R. Fulco, Phys. Rev. Letters **2**, 365 (1959).
[28] F. J. Dyson, Phys. Rev. **99**, 1037 (1955).
[29] G. Takeda, Phys. Rev. **100**, 440 (1955).
[30] Cool, Piccioni, and Clark, Phys. Rev. **103**, 1082 (1956).
[31] S. Barshay, Phys. Rev. **111**, 1651 (1958).
[32] L. S. Rodberg, Phys. Rev. Letters **3**, 58 (1959).